Received: 18 July 2023 | Revised: 6 November 2023 | Accepted: 20 November 2023

DOI: 10.1002/joa3.12970

ORIGINAL ARTICLE

Journal of Arrhythmia Open Access WILEY

The effect of ablation settings on lesion characteristics with DiamondTemp ablation system: An ex vivo experiment

Takehiro Nomura MD[1] | Manabu Maeda MD[1] | Daiki Kumazawa MD[1] | Yosuke Mizuno MD[1] | Kosuke Onodera MD[1] | Shigeru Toyoda MD, PhD[2] | Kennosuke Yamashita MD, PhD, FJCC, FACC, FHRS[1]

[1]Heart Rhythm Center, Department of Cardiovascular Medicine, Sendai Kosei Hospital, Sendai-shi, Miyagi, Japan

[2]Department of Cardiovascular Medicine, School of Medicine, Dokkyo Medical University, Mibu, Tochigi, Japan

Correspondence
Kennosuke Yamashita, 4-15 Hirosemachi, Aoba-ku, Sendai-shi, Miyagi 980-0873, Japan.
Email: kennosuke.atmm3@gmail.com

Abstract

Introduction: Creating large lesion in ablations using the DiamondTemp (DTA) ablation system may reduce the frequency of arrhythmia recurrence and allow the treatment of ventricular arrhythmias. Therefore, this study aimed to investigate whether power, application time, contact force (CF), and contact angle affect lesion formation in the ventricles.

Methods: Ablations were delivered to porcine myocardial preps to evaluate the lesion characteristics. Ablations were conducted with a maximum power of 50 W, target temperature of 58°C, CF of 10, 20, or 30 g, and contact angle between the catheter tip and tissue. The ablation durations were 15, 30, 60 s, 15 s × 2, or 30 s × 2.

Results: Steam pops occurred only in cases with perpendicular contact. The lesion depth was larger in all settings in the perpendicular orientation than in the parallel orientation. The temperatures were lower in all settings in the perpendicular orientation than in the parallel orientation. The lesions became larger as CF increased with perpendicular contact and duration of ≥30 s. The longer application time resulted in larger surface area, depth, and volume of the lesion. Lesion depth was greater with single application of 30 and 60 s than with 15 s × 2 and 30 s × 2, respectively.

Conclusion: It is important to perform a single prolonged application as much as possible to create deeper lesions. Parallel contact with the tissue should be maintained to take advantage of the temperature sensor's capabilities to avoid pop phenomenon.

KEYWORDS
catheter ablation, diamond tip, experimental model, new technology, temperature control

1 | INTRODUCTION

Radiofrequency (RF) ablation is a well-established treatment for cardiac arrhythmias including atrial fibrillation (AF). However, 30% of patients develop AF recurrence after ablation.[1–3] Adequate depth and contiguous lesion formation are necessary for successful AF ablation.[4] Several studies have reported that tissue contact force (CF), contact angle, and ablation indices are useful surrogate measures of optimal lesion formation.[5–8] The novel DiamondTemp ablation (DTA) catheter (Medtronic, Dublin, Ireland), which is a composite-tip, diamond-embedded, temperature-sensing, saline-irrigated RF ablation catheter was designed to allow direct and

This is an open access article under the terms of the Creative Commons Attribution-NonCommercial License, which permits use, distribution and reproduction in any medium, provided the original work is properly cited and is not used for commercial purposes.
© 2023 The Authors. *Journal of Arrhythmia* published by John Wiley & Sons Australia, Ltd on behalf of Japanese Heart Rhythm Society.

rapid measurement of tissue surface temperature and accurate power modulation in a temperature-controlled mode. The DIAMOND-AF trial revealed that the system was non-inferior to CF-sensing RF ablation and have shorter RF durations and procedural times.[9,10] Although CF and contact angle were not provided to the operator, an ex vivo study suggested that CF has little impact on lesion dimensions when applying high power and short durations.[11] However, the effects of CF, contact angle, and long application time on lesion characteristics have not been fully investigated. If deep lesions can develop while reducing the risk of steam pop in the temperature control mode, it may lead to a reduction in the frequency of AF recurrence as a result of reconnection, and DTA may be feasible for the treatment of ventricular arrhythmias. Therefore, this experimental study aimed to investigate whether power, application time, CF, and contact angle affect lesion formation in the ventricles.

2 | METHODS

2.1 | Ablation system

The DTA catheter has an exclusive diamond shunt network, which has a high thermal conductivity that is 200–400 times higher than that of platinum–iridium, and enables rapid catheter tip cooling.[12] The catheter had six external thermocouples, three of which were located on the distal tip, and another three were proximal to the composite RF electrode. The industrial diamond-embedded catheter tip allowed for real-time power titration according to the tip-to-tissue temperature recorded every 20 ms by the generator. These features prevent overheating during RF delivery in a temperature-controlled ablation mode. As saline flows through the diamond network, very little heat is retained, thereby reducing hotspots at catheter tip. The high thermal conductivity and temperature sampling every 20 ms also allow the irrigation to be low flow rate of 8 mL/min. The distal electrode diameter is 0.6 mm and the distance between electrodes is 0.5 mm, allowing high-resolution intra-cardiac potential measurements.

2.2 | Study design and ablation protocol

The ex vivo experimental setup of the DTA system and thermal conditions are shown in Figure 1. Commercially obtained swine hearts excised within 24–72 h were preserved in a fresh state and used for this ex vivo experimental model. The bath was constantly perfused with saline solution at 37°C. While no perfusion was carried out within the myocardium, a circulating saline bath to simulate blood flow. To eliminate the influence of epicardial fat, only the endocardial surface of the porcine heart has been utilized. A stainless steel plate at the bottom of the saline pool was connected to a generator and used as a ground electrode. The catheter irrigation rate is set to the manufacturer's recommended flow rate. That is, 8 mL/min while energized and 2 mL/min when not energized. Ablations were conducted with a maximum power of 50 W, target temperature of 58°C, contact forces (CF) of 10, 20, or

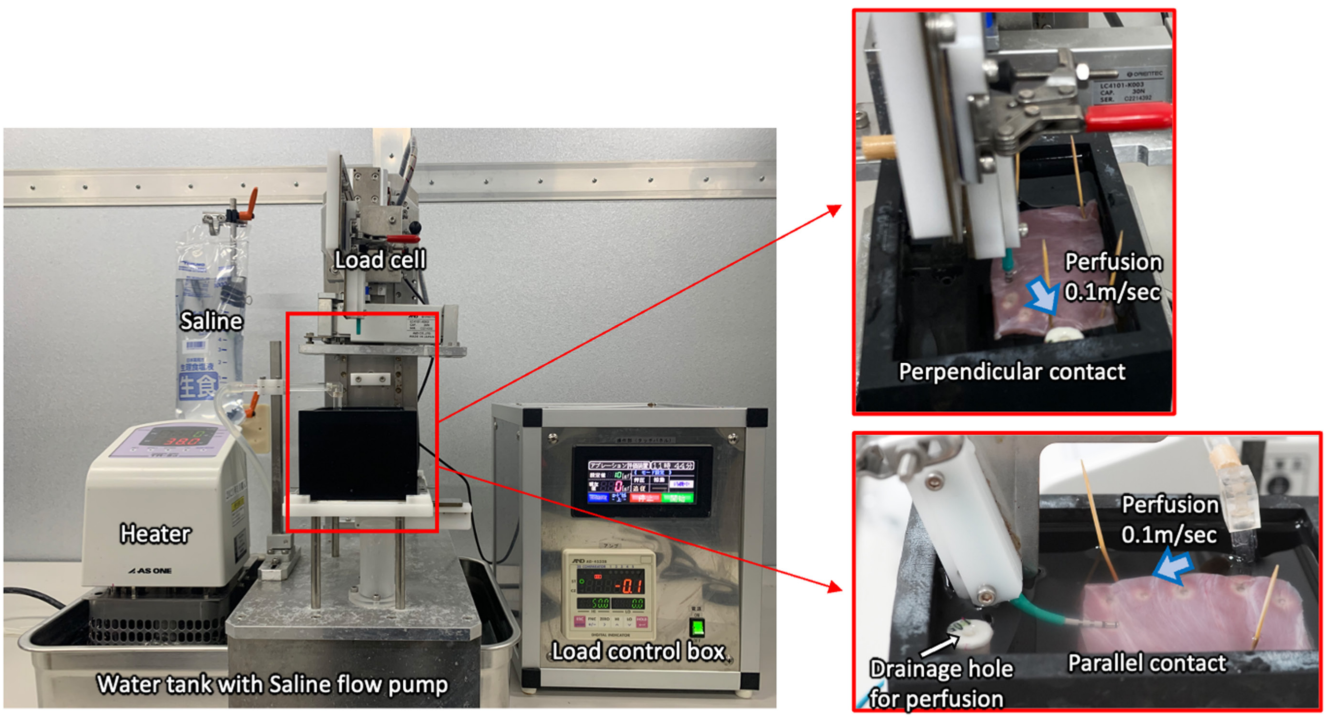

FIGURE 1 Ex vivo experimental model. The saline solution to be perfused was maintained at 37°C. The output and energizing duration were controlled by using the DiamondTemp ablation system (Medtronic, Dublin, Ireland). The DiamondTemp catheter was secured to the introducer and the contact angle and force were maintained.

30 g, and contact angle between the catheter tip and tissue (perpendicular or parallel contact). The ablation durations were 15, 30, or 60 s. Additionally, ablation was performed twice on the same site in 15 or 30 s; repeat ablation on the same site was applied for the same duration after the first delivery of RF in 15 or 30 s. In the present study, the two applications for 15 and 30 s were denoted as "15 × 2 s" and "30 × 2 s", respectively. The CF was accurately maintained using a load control box, which automatically controlled the CF obtained from the load cell that held the catheter (Figure 1). The myocardial thickness ranges from 10–15 mm and four lesions were created for each setting. Each lesion was measured with a digital caliper with a resolution of 0.1 mm by two different observers blinded to the lesion protocol. We evaluate the lesion characteristics (surface length and width, maximum depth and width, depth to maximum length, surface area, and volume) (Figure 2), generator impedance drop during RF delivery, steam-pop incidence, and maximum and minimum temperatures. "Maximum temperature" means a maximum temperature during application, whereas "minimum temperature" means minimum value of the six thermocouples at the moment the "maximum temperature" is recorded at any electrode during a RF delivery. Temperature data were extracted every second, although they were recorded every 20 ms using the DTA generator system. The variables were compared based on the ablation duration, CF, and contact angle. For simplicity, the ablation settings were as follows: if the CF was 30 g, the perpendicular angle and duration were 15 s, then 30 g/perp/15 s.

2.3 | Statistical analyses

All statistical analyses were conducted using the JMP software (version 16.0; SAS Institute, Inc., Cary, NC, USA). Continuous variables are presented as medians and interquartile ranges. The Mann–Whitney U and Kruskal–Wallis tests were used to assess significant differences in continuous variables. Categorical variables are described as frequencies and percentages. The chi-square test was used to compare categorical variables. Statistical significance was set at $p < .05$.

3 | RESULTS

3.1 | Difference in lesions among CFs

Altogether, 120 lesions were analyzed in the present study. The prepared myocardial thickness was 11.6 mm (11.0–12.6). Of the 80 lesions created by single RF application, the temperature-based power titration mode worked in 74 lesions. The measured variables are listed in Table 1. The lesion depth and volume were significantly larger in the setting with a CF of 30 g than in the setting with a CF of 10 g when the energizing durations were 30 and 60 s, but not for a duration of 15 s in the perpendicular orientation. The surface area was significantly larger in the setting with a CF of 30 g than in the setting with a CF of 10 g for all the energizing durations.

In the parallel contact group, there were no significant differences in lesion diameter, depth, surface area, or volume among the CFs. The only significant difference was found in the depth of maximum width, which was approximately 0.1–0.2 mm.

3.2 | Difference by contact angle

The depth of the lesions was relatively larger in all settings in the perpendicular orientation than in the parallel orientation, and the difference was 0.2–2.0 mm. The surface area was larger with perpendicular contact in 12 (80.0%) cases, except for 10, 10, and 20 g/15 s. The maximum and minimum temperatures were lower in all settings in the perpendicular orientation than in the parallel orientation, and the difference was significant in seven (46.7%) and six (40.0%), respectively.

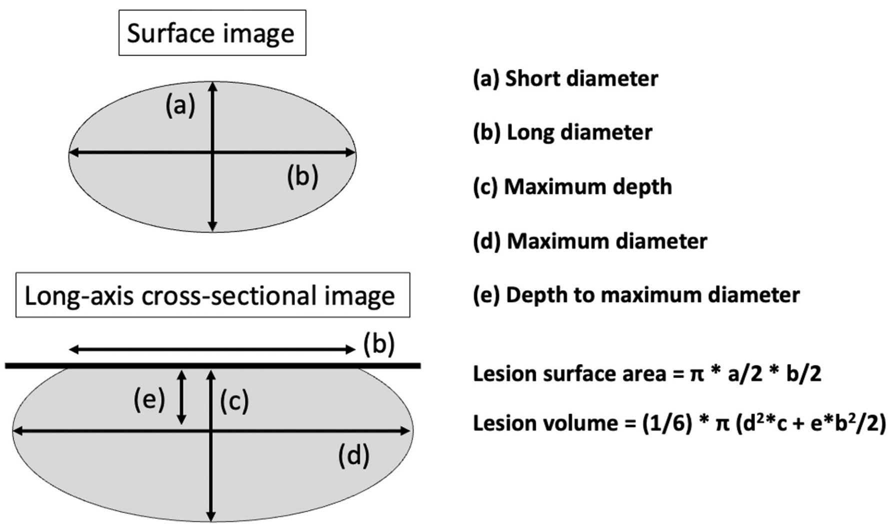

FIGURE 2 Schema of the surface and long-axis cross-section of the lesions. Surface area and lesion volume were calculated using the following formula: surface area $= \pi \times a/2 \times b/2$; and lesion volume $= (1/6) \times \pi \times (e2 \times d + c \times a2/2)$.

TABLE 1 Lesion size and change in resistance and temperature during energization per contact force.

Perpendicular orientation					
Application duration, s	**15**				**30**
Contact force, g	**10 (*n* = 4)**	**20 (*n* = 4)**	**30 (*n* = 4)**	***p* value**	**10 (*n* = 4)**
Long diameter, mm	7.2 (6.1–7.6)	7.0 (6.7–7.3)	7.4 (7.3–7.6)	.199	6.8 (6.6–7.1)
Short diameter, mm	5.9 (5.4–6.1)	6.6 (5.6–7.0)	7.1 (6.8–7.2)	.030	6.6 (6.5–6.6)
Depth, mm	4.3 (4.1–4.4)	4.5 (3.9–4.7)	4.5 (4.2–4.6)	.471	5.6 (5.5–5.6)
Maximum width, mm	8.1 (7.9–8.4)	8.2 (8.0–8.5)	8.5 (8.1–9.3)	.276	9.5 (9.2–10.0)
Depth of maximum width, mm	1.6 (1.5–1.7)	1.8 (1.7–2.1)	1.8 (1.8–2.2)	.036	2.0 (1.9–2.0)
Surface area, mm^2	34.3 (26.1–35.4)	35.4 (30.2–39.6)	40.9 (40.1–41.9)	.030	35.3 (34.2–36.8)
Volume, mm^3	171.1 (150.3–183.3)	183.2 (157.4–195.6)	195.0 (172.4–233.9)	.246	287.6 (271.2–313.0)
Steam pop, *n* (%)	0 (0%)	0 (0%)	0 (0%)	N/A	3 (75%)
Initial impedance, Ohm	81.0 (77.8–82.0)	82.5 (81.0–82.8)	81.0 (80.3–82.5)	.590	81.5 (77.8–83.8)
Minimum impedance, Ohm	72.5 (71.3–74.5)	72.0 (70.5–72.8)	77.0 (75.3–78.9)	.025	71.0 (71.0–73.3)
Impedance drop, Ohm	14.0 (13.3–14.8)	13.5 (12.3–14.8)	13.0 (12.0–14.0)	.467	12.5 (11.3–13.0)
Impedance drop, %	16.2 (15.1–17.2)	15.7 (14.5–17.3)	14.4 (13.4–15.4)	.161	14.7 (13.5–15.5)
Maximum temperature, °C	61.0 (60.6–61.2)	59.2 (58.9–60.3)	59.5 (59.3–59.7)	.032	60.3 (59.2–60.5)
Minimum temperature, °C	53.7 (53.5–53.7)	53.3 (53.1–53.9)	51.2 (48.0–53.3)	.095	55.4 (54.5–56.5)
Total energy, J	720 (676–744)	600 (576–656)	596 (585–613)	.025	1497 (1233–1499)
Parallel orientation					
Application duration, s	**15**				**30**
Contact force, g	**10 (*n* = 4)**	**20 (*n* = 4)**	**30 (*n* = 4)**	***p* value**	**10 (*n* = 4)**
Long diameter, mm	7.7 (7.4–7.9)	7.6 (7.2–7.7)	7.7 (7.4–8.1)	.584	7.5 (7.2–8.0)
Short diameter, mm	6.1 (6.0–6.2)	6.7 (6.5–7.0)	6.3 (5.9–6.4)	.031	6.5 (6.4–6.6)
Depth, mm	4.1 (3.8–4.3)	4.5 (4.3–4.6)	4.2 (4.1–4.4)	.092	5.0 (4.9–5.2)
Maximum width, mm	8.5 (8.0–9.2)	9.1 (8.5–9.4)	8.7 (8.4–9.0)	.351	10.6 (9.6–11.5)
Depth of maximum width, mm	1.5 (1.4–1.6)	1.8 (1.6–1.9)	1.7 (1.6–1.9)	.039	2.1 (1.9–2.5)
Surface area, mm^2	36.6 (35.5–38.1)	39.6 (39.0–40.4)	37.3 (36.3–39.0)	.044	38.0 (36.7–41.6)
Volume, mm^3	172.4 (157.9–210.0)	223.3 (193.1–234.6)	196.1 (182.2–207.9)	.138	319.7 (273.1–402.7)
Steam pop, *n* (%)	0 (0%)	0 (0%)	0 (0%)	N/A	0 (0%)
Initial impedance, Ohm	86.5 (86.0–87.8)	85.0 (84.3–86.5)	90.0 (87.8–92.3)	.027	84.0 (82.5–85.5)
Minimum impedance, Ohm	67.5 (64.5–69.8)	69.5 (69.0–70.0)	71.0 (70.0–73.0)	.045	68.0 (65.3–70.8)
Impedance drop, Ohm	13.0 (12.3–13.8)	12.0 (12.0–12.0)	10.5 (9.3–12.5)	.102	13.0 (12.3–13.8)
Impedance drop, %	16.4 (14.9–17.4)	14.8 (14.7–15.5)	13.0 (11.5–15.1)	.077	15.6 (15.5–17.0)
Maximum temperature, °C	59.6 (59.2–59.9)	60.2 (59.8–60.8)	60.8 (60.1–61.4)	.036	59.3 (58.9–60.3)
Minimum temperature, °C	55.9 (54.3–56.3)	55.0 (54.7–56.8)	55.5 (55.2–56.2)	.779	54.3 (53.2–55.7)
Total energy, J	594 (545–693)	519 (494–539)	493 (487–514)	.015	1190 (1044–1377)

3.3 | Difference in lesions among the RF durations

In all settings, the lesion depth increased with energization durations of 15, 30, and 60 s in that order. Figure 3 showed the original image of the lesion, as the diameter and depth of the lesions. The Kruskal–Wallis test showed that the differences were statistically significant among the RF durations. The surface area at 10, 20, 30, and 10 g/perp also increased with increasing energization duration. At 20 and 30 g/parallel, the surface area was greater in a setting with a duration of 60 s than that with a duration of 15 and 30 s, but no significant differences were observed between 15 and 30 s (Figure 4).

3.4 | Difference between two-time and single applications

The lesion depth was greater with a duration of 30 s than with a duration of 15 s × 2, except for 30 g/perp, and the difference was statistically significant at 10 g/perp and 10 g/parallel (Table 2). Conversely,

			60			
20 ($n=4$)	30 ($n=4$)	p value	10 ($n=4$)	20 ($n=4$)	30 ($n=4$)	p value
8.7 (8.4–9.1)	8.7 (7.9–8.9)	.024	8.0 (8.0–8.1)	9.2 (8.5–10)	9.0 (8.9–9.2)	.022
8.0 (7.8–8.2)	8.3 (7.6–8.6)	.023	7.5 (7.5–8.0)	8.8 (8.0–9.4)	8.8 (8.5–9.2)	.039
6.0 (5.7–6.5)	6.1 (6.0–6.2)	.023	7.4 (7.3–7.9)	8.0 (7.1–8.5)	7.2 (7.2–7.3)	.217
9.8 (9.6–10.1)	10.2 (10.0–10.6)	.092	10.5 (10.2–10.5)	11.2 (10.7–11.4)	11.8 (11.4–12.6)	.011
2.3 (2.2–2.8)	2.0 (2.0–2.1)	.023	2.1 (2.1–2.1)	2.2 (2.0–2.3)	2.2 (2.2–2.3)	.107
54.5 (52.1–58.4)	56.8 (47.6–58.9)	.024	47.0 (46.8–50.9)	64.2 (53.4–73.3)	61.9 (59.5–66.4)	.038
361.2 (323.8–378.3)	369.2 (355.5–400.3)	.035	461.5 (432.6–486.8)	557.6 (490.3–625.4)	576.1 (531.5–650.0)	.031
0 (0%)	1 (25%)	.043	3 (75%)	3 (75%)	3 (75%)	1
78.0 (77.0–80.5)	81.5 (81.0–82.0)	.158	82.0 (77.3–84.5)	84.5 (81.0–85.0)	79.5 (77.5–82.3)	.186
71.0 (70.0–72.3)	74.0 (74.0–74.8)	.035	71.0 (70.3–71.0)	70.0 (62.5–71.5)	73.0 (73.0–73.0)	.016
12.0 (11.3–12.8)	12.0 (9.8–15.0)	.905	13.0 (11.5–13.0)	11.5 (11.0–21.8)	15.5 (13.0–19.5)	.267
14.6 (13.5–15.1)	14.0 (11.3–16.8)	.838	15.5 (13.9–15.6)	14.1 (13.3–25.7)	17.4 (15.1–22.8)	.498
59.4 (59.0–59.8)	59.3 (58.9–59.7)	.263	58.4 (57.8–59.3)	59.5 (58.9–60.1)	59.6 (57.7–60.8)	.524
53.7 (52.9–54.2)	52.5 (49.3–54.9)	.058	54.8 (53.2–55.3)	53.1 (51.5–54.5)	51.6 (49.3–52.6)	.048
1385 (1321–1419)	1394 (1188–1450)	.310	2947 (2487–2998)	2784 (2326–2862)	2893 (2718–2950)	.280

			60			
20 ($n=4$)	30 ($n=4$)	p value	10 ($n=4$)	20 ($n=4$)	30 ($n=4$)	p value
7.9 (7.7–8.1)	7.3 (7.1–7.6)	.118	7.8 (7.5–7.9)	8.2 (7.4–9.1)	8.4 (8.2–8.9)	.225
6.4 (6.0–6.8)	6.5 (5.9–6.5)	.874	7.2 (7.0–7.4)	7.3 (7.0–7.6)	7.4 (7.1–8.2)	.688
5.4 (5.3–5.6)	5.3 (5.0–5.5)	.046	6.4 (6.2–6.5)	6.0 (5.5–6.3)	6.9 (6.5–7.0)	.065
9.5 (9.4–9.9)	9.9 (9.6–10.4)	.138	10.3 (9.8–10.5)	9.6 (8.9–10.7)	11.4 (10.7–11.6)	.134
1.9 (1.8–2.0)	2.3 (2.2–2.3)	.037	2.3 (2.2–2.4)	2.1 (2.0–2.2)	2.4 (2.2–2.5)	.020
39.0 (37.6–43.0)	36.4 (34.0–38.4)	.138	44.3 (40.9–45.3)	47.9 (41.4–52.4)	48.1 (46.5–57.1)	.119
291.1 (283.5–303.3)	297.8 (292.9–326.1)	.437	386.1 (352.0–411.2)	312.6 (280.4–403.2)	500.0 (455.9–527.5)	.055
0 (0%)	0 (0%)	N/A	0 (0%)	0 (0%)	0 (0%)	N/A
83.0 (82.0–84.8)	86.0 (86.0–89.0)	.034	83.5 (82.3–84.0)	82.5 (81.3–84.5)	86.0 (84.5–89.8)	.051
67.5 (67.0–68.0)	69.5 (69.0–70.0)	.237	67.5 (64.5–71.3)	70.0 (69.0–71.8)	68.5 (68.0–69.0)	.244
10.5 (9.3–13.3)	12.0 (12.0–12.0)	.143	11.0 (9.3–13.5)	13.0 (11.3–15.5)	13.5 (12.3–14.8)	.288
13.5 (12.0–16.4)	14.7 (14.6–14.8)	.076	13.8 (11.9–16.4)	15.4 (13.9–18.2)	16.3 (15.4–18.1)	.287
60.4 (60.2–60.8)	60.5 (60.2–61.1)	.157	60.2 (60.0–60.6)	60.1 (59.7–60.4)	59.9 (59.0–60.2)	.308
54.2 (53.5–57.0)	55.9 (54.7–57.4)	.298	55.9 (53.1–56.4)	54.9 (52.6–60.0)	55.9 (54.2–56.4)	.542
880 (844–897)	828 (808–873)	.018	2202 (1823–2511)	1634 (1546–1714)	1505 (1472–1587)	.013

the depth was significantly greater with a duration of 15 s × 2 at 30 g/perp. The surface area was significantly larger with a duration of 30 s than with a duration of 15 s × 2 for 10 g/perp, 20 g/perp, and 20 g/parallel. Conversely, the surface area was larger with the duration of 15 s × 2 in the 10 and 30 g/parallel conditions, but the difference was not statistically significant.

The lesion depth was larger in settings with a duration of 60 s than in those with a duration of 30 s × 2 in all settings, except for 30 g/perp, and the difference was statistically significant at 10 g/perp. Although the surface area was greater at a 60 s energization duration than at a 30 s × 2 energization duration for all settings, except for 10 g/parallel, this difference was not statistically significant.

3.5 | Characteristics of RF application with steam pop

A steam pop occurred in 21 (35.0%) out of the 60 lesions with perpendicular contact. However, no pops were observed with the ablation

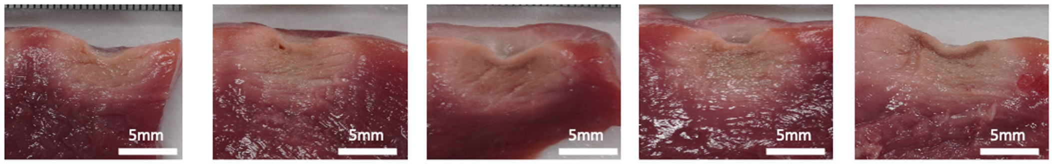

Perpendicular	15sec	15sec×2	30sec	30sec×2	60sec
Long Diameter, mm	7.0 (6.7–7.3)	7.2 (6.5–7.8)	8.7 (8.4–9.1)	8.8 (7.8–9.4)	9.2 (8.5–10)
Lesion Depth, mm	4.5 (3.9–4.7)	5.8 (5.5–5.9)	6.0 (5.7–6.5)	7.4 (7.1–9.2)	8.0 (7.1–8.5)

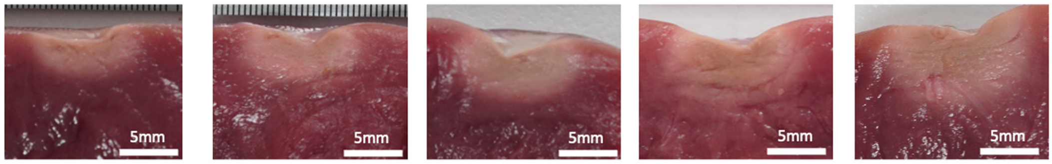

Parallel	15sec	15sec×2	30sec	30sec×2	60sec
Long Diameter, mm	7.6 (7.2–7.7)	7.1 (6.4–7.6)	7.9 (7.7–8.1)	7.4 (7.3–7.8)	8.2 (7.4–9.1)
Lesion Depth, mm	4.5 (4.3–4.6)	5.2 (4.7–5.4)	5.4 (5.3–5.6)	5.8 (5.6–5.9)	6.0 (5.5–6.3)

FIGURE 3 An example of the appearance of a lesion categorized by the application durations and the catheter contact orientations.

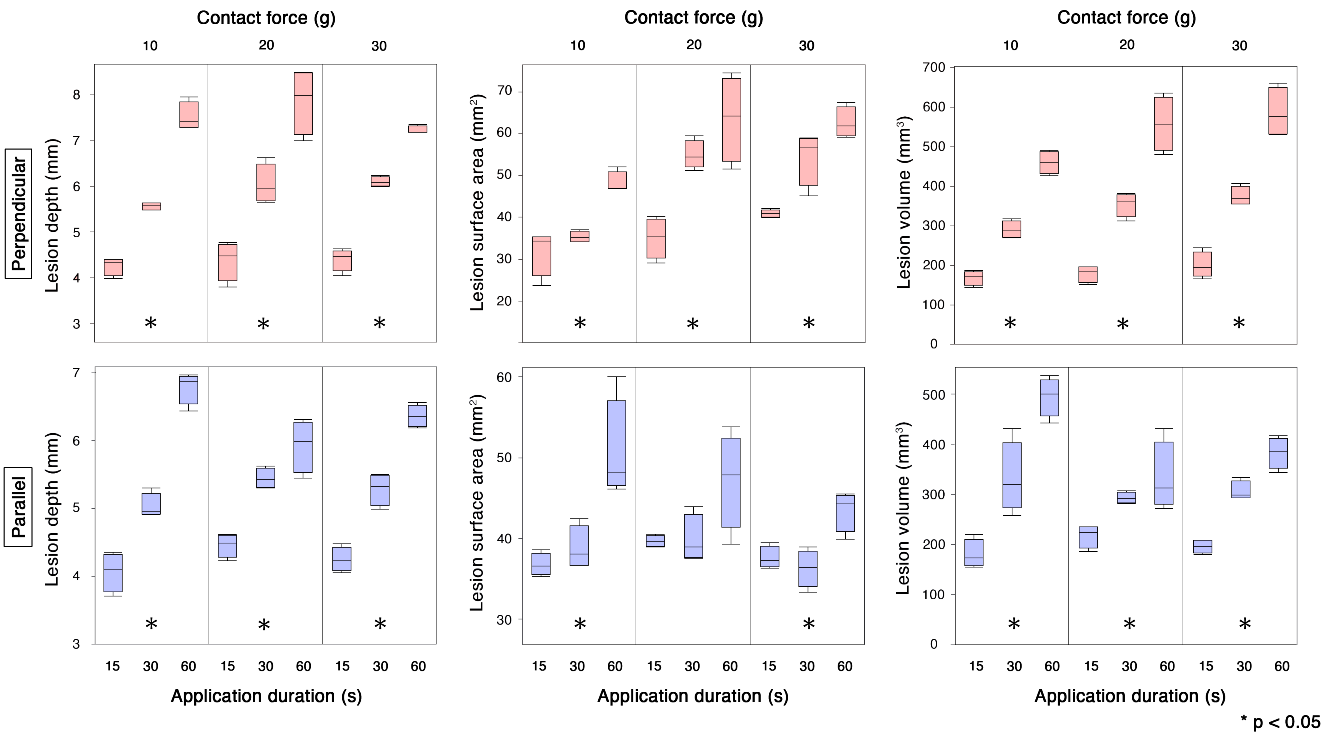

FIGURE 4 Box-and-whisker diagram showing the relationship between energization time and lesion size. In all settings, the lesion depth increased with energization durations of 15, 30, and 60 s in that order except for the surface area with a contact force of 20 g and parallel contact angle. The Kruskal–Wallis test showed that the differences were statistically significant.

duration of 15 s. On the other hand, it did not occur in those with parallel contact, regardless of the application duration. A comparison of lesions with and without the pop phenomenon showed that the time to reach the set temperature limit of 58°C was significantly longer for lesions with the pop phenomenon (9.0 s [5.0–18.0] vs. 3.0 s [3.0–5.0], $p < .001$). The maximum temperature did not reach 58°C in six (28.6%) of the 21 lesions with steam pop, and the average output during energization was higher in lesions with steam pop (30 s, 40.0 W [27.4–40.0] vs. 50.0 W [50.0–50.0], $p < .001$; 60 s, 35.0 W [24.1–40.0] vs. 50.0 W [49.4–50.0], $p < .001$). The difference in baseline generator impedance between with and without steam pop was not significant (84.0 Ω [82.5–86.0] vs. 83.0 Ω [81.0–85.0], $p = .095$).

TABLE 2 Comparison of lesion size between the application durations of 15 s × 2 and 30 s and between 30 s × 2 and 60 s.

	15 s × 2	30 s	*p* value	30 s × 2	60 s	*p* value
10 g						
Perpendicular						
Surface area, mm²	26.9 (26.4–27.1)	35.3 (34.2–36.8)	.03	46.1 (44.9–52.2)	47.0 (46.8–50.9)	.63
Lesion volume, mm³	220.7 (209.9–231.9)	287.6 (271.2–313.0)	.03	431.4 (384.5–439.2)	461.5 (432.6–486.8)	.11
Parallel						
Surface area, mm²	41.7 (40.0–41.8)	38.0 (36.7–41.6)	.29	45.8 (42.4–47.7)	48.1 (46.5–57.1)	.11
Lesion volume, mm³	218.3 (117.5–230.3)	319.7 (273.1–402.8)	.03	400.0 (344.4–516.4)	500.0 (455.9–527.5)	.49
20 g						
Perpendicular						
Surface area, mm²	39.4 (32.0–43.4)	54.5 (52.1–58.4)	.03	58.7 (43.9–66.3)	64.2 (53.4–73.3)	.34
Lesion volume, mm³	244.8 (217.5–252.1)	361.2 (323.8–378.3)	.03	395.5 (335.3–578.2)	557.6 (490.3–625.4)	.2
Parallel						
Surface area, mm²	32.8 (29.8–32.9)	39.0 (37.6–43.0)	.03	39.4 (38.6–40.1)	47.9 (41.4–52.4)	.14
Lesion volume, mm³	235.1 (218.1–258.3)	291.1 (283.5–303.3)	.03	406.8 (375.8–414.4)	312.6 (280.4–403.2)	.34
30 g						
Perpendicular						
Surface area, mm²	52.3 (50.0–54.5)	56.8 (47.6–58.9)	.34	60.8 (58.5–63.7)	61.9 (59.5–66.4)	.49
Lesion volume, mm³	406.0 (393.3–432.6)	369.2 (355.5–400.3)	.11	609.5 (573.3–758.7)	576.1 (531.5–650.0)	.49
Parallel						
Surface area, mm²	40.1 (37.1–45.5)	36.4 (34.0–38.4)	.2	47.9 (45.2–50.7)	44.3 (40.9–45.3)	.057
Lesion volume, mm³	227.7 (204.7–241.0)	297.8 (292.9–326.1)	.03	357.1 (332.7–403.3)	386.1 (352.0–411.2)	.49

4 | DISCUSSION

This study aimed to investigate whether power, application time, CF, and contact angle affect lesion formation in the ventricles. The experiment demonstrates some interesting observations. First, CF had an effect on lesion size only when the application duration was more than 30 s and the contact angle was perpendicular. Second, a deeper lesion developed in cases with a perpendicular contact and steam pops occurred only when the contact angles were perpendicular. Third, a single prolonged energization was associated with larger lesions compared to a double shorter energization.

4.1 | Effect of CF

In this experiment, as in previous reports, there was no significant difference in either depth or surface area with increasing CF for a short duration of 15 s.[11] However, the lesions became larger as the CF increased when the contact angle was perpendicular and the duration was >30 s. Although the difference was not significant in the cases with parallel contact, the depth and surface area were always greater when the CF was 30 g than when it was 10 g. These results suggest that CF may influence the lesion size even with DTA if the energization duration is ≥30 s, as previously reported for CF-sensing ablation catheters.[5–8,13,14]

4.2 | Effect of contact angle on lesion size

A previous clinical or ex vivo experimental study reported that lesions were smaller and shallower with perpendicular contact.[15,16] Contrarily, in an ex vivo experimental study, a deeper lesion developed in cases with a perpendicular contact.[17] In the perpendicular contact, the output control by the temperature control system started to limit later than in the parallel contact in the experiment, and therefore, higher currents were delivered until the temperature limit.[18] It is possible that the DTA catheter had six thermocouples located at the distal tip and proximal site. Therefore, in perpendicular contact, the thermocouples at the proximal tip are not in contact with the tissue, whereas in parallel contact, one or two sensors at the proximal tip are in contact with the tissue and may reflect the tissue temperature more accurately.

4.3 | Effect of longer RF delivery

Under similar CF and contact angle conditions, the surface area, depth, and volume of the lesion increased with longer application times. Therefore, extending the energization duration may be effective in creating deeper and larger volumes, particularly for the ablation of ventricular arrhythmias. Recently, it has been repeatedly reported that deeper lesions develop with standard ablation therapies rather than with therapies with high power and short duration[19,20] and these results are not surprising, as longer energization duration allows for deeper and larger lesion creation. However, our study showed that steam pops occurred at an energization duration of ≥30s with a perpendicular contact. If the angle of contact with the tissue can be recognized by fluoroscopy or 3D mapping, it may be possible to extend the energization duration more safely using the DTA catheter.

4.4 | Comparison between one-time application with a long duration or two-time application with a short duration

First, in the comparison between the 60s and 30s×2 settings, deeper lesions developed with a duration of 60s in five of the six settings. Similarly, in the comparison of 30s and 15s×2, deeper lesions developed in five of the six settings. For all lesions, a two-time application consistently resulted in larger lesions than a single application. This can likely be attributed to the initial conduction causing thermal changes in the tissue, which leads to a reduction in the local impedance of the lesioned area. As a result, during the second application, with the increased thermal conductivity from the previous conduction, the electric current penetrates more deeply and widely, potentially leading to an expanded lesion size. On the other hand, when comparing 15s×2 each to a single 30s application, the latter results in a larger lesion size. This is because, the tissue undergoes interim cooling between sessions with the two 15s×2 applications, whereas a continuous 30s application promotes a more substantial rise in tissue temperature.

4.5 | Steam pop with perpendicular contact angle

Steam pops occurred only when the contact angles were perpendicular, not when they were parallel. The measured maximum and minimum temperatures were always lower when the contact angle was perpendicular than when the contact angle was parallel. Therefore, the tissue temperature assumed from the six thermocouples is likely to be underestimated with the perpendicular contact, resulting in inadequate output control and failure to suppress the steam pop. In a perpendicular contact, the distal three electrodes were in contact with the tissue, but the remaining three proximal electrodes placed were not. This may result in not reflecting the tissue temperature accurately. Furthermore, the distal electrodes were close to the catheter's irrigation hole. If cooled by the catheter's irrigation, there might be a delay in the feedback of tissue temperature. While there was no observed difference in the change of impedance between ablations with and without a pop, the baseline impedance in parallel contact was displayed as approximately 5Ω higher than that in the perpendicular contact group. This is because of the influence of the electrode surface area in contact with the tissue. It is believed that this resulted in a difference in the amount of current flowing into the tissue during ablation, which may have led to the difference in the frequency of pops. The association between CF and lesion size was more apparent with the perpendicular contact, which may also be related to the differences in temperature control.

5 | LIMITATIONS

This ex vivo model cannot be directly applied to actual clinical practice. The conditions of excised porcine myocardium and lesions would be different from beating hearts. In this set of experiments, all tests with perpendicular contact were conducted first, followed by lesion creation with parallel contact. Consequently, the myocardium used for parallel contact had been stored for approximately 3–4h longer. Therefore, it is concluded that there are no significant issues regarding the experimental material. Moreover, the DTA catheter did not have a CF sensor, and evaluating the CF at 10, 20, and 30g is impossible. The same is true for the contact angle, which is more reproducible and accurate than that produced by fluoroscopic guidance and catheter manipulation. Ideally, a more detailed evaluation would be possible if in vivo model experiments were performed under conditions where a corresponding 3D mapping system is present and the CF force and contact angle were displayed.

In addition, only four lesions in each ablation mode were created in the experiment. Therefore, this study alone might be statistically underpowered to demonstrate differences among conditions. Additional research may be necessary. This study evaluated only 50W but did not examine whether 30 or 40W could create a deeper lesion more safely as compared with 50W. Generally, it is thought that a long application of 30 or 40W with a high CF is the best way for creating the deepest lesion without pop phenomenon, but we have no information on this. However, no pop was found in any setting with parallel contact; therefore, it is possible that a long application with 50W parallel contact for 60s or more could create deeper and larger lesions than those created with conventional catheters.

6 | CONCLUSION

To optimize the DTA catheter, it is crucial to manipulate both the distal and proximal thermocouples in close contact with the tissue in a parallel orientation. When temperature control is properly and power titration is accurately applied, it allows for a longer application without inducing pop phenomenon in the tissue.

AUTHOR CONTRIBUTIONS
Takehiro Nomura and Kennosuke Yamashita devised the study design and concepts. Takehiro Nomura and Kennosuke Yamashita analyzed and interpreted the data. Takehiro Nomura drafted the manuscript. Manabu Maeda, Daiki Kumazawa, Yosuke Mizuno, Kosuke Onodera, Shigeru Toyoda and Kennosuke Yamashita performed critical revision for important intellectual content. All authors approved the final version of the manuscript.

CONFLICT OF INTEREST

Authors declare no conflict of interests for this article.

DATA AVAILABILITY STATEMENT

Raw data were generated at Sendai Kousei Hospital. Derived data supporting the findings of this study are available from the corresponding author T.N. on request.

ETHICS STATEMENT

The ethical committee of Sendai Kousei Hospital waived the requirement for obtaining ethical approval because this research was neither a clinical study nor an animal experiment.

ORCID

Takehiro Nomura https://orcid.org/0000-0003-4826-2184

REFERENCES

1. Nedios S, Kosiuk J, Koutalas E, Kornej J, Sommer P, Arya A, et al. Comparison of left atrial dimensions in CT and echocardiography as predictors of long-term success after catheter ablation of atrial fibrillation. J Interv Card Electrophysiol. 2015;43:237–44.
2. Watanabe R, Nagashima K, Wakamatsu Y, Otsuka N, Yokoyama K, Matsumoto N, et al. Different determinants of the recurrence of atrial fibrillation and adverse clinical events in the mid-term period after atrial fibrillation ablation. Circ J. 2022;86:233–42.
3. Marrouche NF, Wilber D, Hindricks G, Jais P, Akoum N, Marchlinski F, et al. Association of atrial tissue fibrosis identified by delayed enhancement MRI and atrial fibrillation catheter ablation: the DECAAF study. JAMA. 2014;311:498–506.
4. El Haddad M, Taghji P, Phlips T, Wolf M, Demolder A, Choudhury R, et al. Determinants of acute and late pulmonary vein reconnection in contact force-guided pulmonary vein isolation: identifying the weakest link in the ablation chain. Circ Arrhythm Electrophysiol. 2017;10:e004867. https://doi.org/10.1161/CIRCEP.116.004867
5. Yokoyama K, Nakagawa H, Shah DC, Lambert H, Leo G, Aeby N, et al. Novel contact force sensor incorporated in irrigated radiofrequency ablation catheter predicts lesion size and incidence of steam pop and thrombus. Circ Arrhythm Electrophysiol. 2008;1:354–62.
6. Thiagalingam A, D'Avila A, Foley L, Guerrero JL, Lambert H, Leo G, et al. Importance of catheter contact force during irrigated radiofrequency ablation: evaluation in a porcine ex vivo model using a force-sensing catheter. J Cardiovasc Electrophysiol. 2010;21:806–11.
7. Sulkin MS, Laughner JI, Hilbert S, Kapa S, Kosiuk J, Younan P, et al. Novel measure of local impedance predicts catheter-tissue contact and lesion formation. Circ Arrhythm Electrophysiol. 2018; 11:e005831.
8. Yamashita K, Kamali R, Kwan E, MacLeod RS, Dosdall DJ, Ranjan R. Effective ablation settings that predict chronic scar after left atrial ablation. JACC Clin Electrophysiol. 2020;6:143–52.
9. Starek Z, Lehar F, Jez J, Pesl M, Neuzil P, Sediva L, et al. Efficacy and safety of novel temperature-controlled radiofrequency ablation system during pulmonary vein isolation in patients with paroxysmal atrial fibrillation: TRAC-AF study. J Interv Card Electrophysiol. 2022;64:375–81.
10. Kautzner J, Albenque J-P, Natale A, Maddox W, Cuoco F, Neuzil P, et al. A novel temperature-controlled radiofrequency catheter ablation system used to treat patients with paroxysmal atrial fibrillation. JACC Clin Electrophysiol. 2021;7:352–63.
11. Verma A, Schmidt MM, Lalonde J-P, Ramirez DA, Getman MK. Assessing the relationship of applied force and ablation duration on lesion size using a diamond tip catheter ablation system. Circ Arrhythm Electrophysiol. 2021;14:e009541.
12. Iwasawa J, Koruth JS, Petru J, Dujka L, Kralovec S, Mzourkova K, et al. Temperature-controlled radiofrequency ablation for pulmonary vein isolation in patients with atrial fibrillation. J Am Coll Cardiol. 2017;70:542–53.
13. Nakagawa H, Ikeda A, Sharma T, Govari A, Ashton J, Maffre J, et al. Comparison of in vivo tissue temperature profile and lesion geometry for radiofrequency ablation with high power-short duration and moderate power-moderate duration: effects of thermal latency and contact force on lesion formation. Circ Arrhythm Electrophysiol. 2021;14:e009899.
14. Yamashita K, Ghafoori E, Silvernagel J, Ashton J, J Dosdall D, MacLeod R, et al. The effective contact force to minimize edema relative to chronic lesion formation during radiofrequency ablation in ventricular wall. Int Heart J. 2019;60:1407–14.
15. Ohta M, Hayashi K, Sato H, Noto T, Kawahatsu K, Katagiri M, et al. Impact of catheter contact angle on lesion formation and durability of pulmonary vein isolation. J Interv Card Electrophysiol. 2022;64:677–85.
16. Calzolari V, De Mattia L, Basso F, Crosato M, Scalon A, Squasi PAM, et al. Ablation catheter orientation: in vitro effects on lesion size and in vivo analysis during PVI for atrial fibrillation. Pacing Clin Electrophysiol. 2020;43:1554–63.
17. Masnok K, Watanabe N. Catheter contact area strongly correlates with lesion area in radiofrequency cardiac ablation: an ex vivo porcine heart study. J Interv Card Electrophysiol. 2022;63:561–72.
18. Eick OJ. Factors influencing lesion formation during radiofrequency catheter ablation. Indian Pacing Electrophysiol J. 2003;3:117–28.
19. Bourier F, Duchateau J, Vlachos K, Lam A, Martin CA, Takigawa M, et al. High-power short-duration versus standard radiofrequency ablation: insights on lesion metrics. J Cardiovasc Electrophysiol. 2018;29:1570–5.
20. Takigawa M, Kitamura T, Martin CA, Fuimaono K, Datta K, Joshi H, et al. Temperature- and flow-controlled ablation/very-high-power short-duration ablation vs conventional power-controlled ablation: comparison of focal and linear lesion characteristics. Heart Rhythm. 2021;18:553–61.

How to cite this article: Nomura T, Maeda M, Kumazawa D, Mizuno Y, Onodera K, Toyoda S, et al. The effect of ablation settings on lesion characteristics with DiamondTemp ablation system: An ex vivo experiment. J Arrhythmia. 2024;40:109–117. https://doi.org/10.1002/joa3.12970